Electronic Supplementary Material (ESI) for Green Chemistry.

Air atmospheric photocatalytic oxidation by ultrathin C, N-TiO_2 nanosheets

Xiuyan Cheng,[a,b] Jianling Zhang,*[a,b,c] Lifei Liu,[a,b] Lirong Zheng,[d] Fanyu Zhang,[a,b] Ran Duan,[e] Yufei Sha,[a,b] Zhuizhui Su[a,b] and Fei Xie[d]

Correspondence to: zhangjl@iccas.ac.cn (Jianling Zhang).

1. Materials and Methods

Materials. Titanium(IV) *n*-butoxide ($Ti(OC_4H_9)_4$, 99% purity), 2-aminoterephthalic acid (NH_2-H_2BDC, A.R. grade) and methyl sulfoxide-d6 (DMSO-d6, 99.8%) were provided by InnoChem Science & Technology Co., Ltd. *N*,*N*-dimethylformamide (DMF) and methanol (A.R. grade) were supplied by Beijing Chemical Works. P25 was obtained from Acros Organic of Thermo Fisher Scientific Co., Ltd. Acetonitrile (A.R. Grade), anhydrous methyl alcohol (CH_3OH, A.R. Grade) and ethanol (A.R. Grade) were purchased from Beijing Chemical Works. Deionized water and oxygen (O_2, >99.9%) were provided by Beijing Analysis Instrument Factory. 1,3,5-trioxane was purchased from Jilin Yanshen Technology Co., Ltd. Nafion D-521 dispersion (5% w/w in water and 1-propanol, ≥ 0.92 meq/g exchange capacity) was purchased from Alfa Aesar China Co., Ltd.

Synthesis of NH_2-MIL-125. NH_2-H_2BDC (3.26 g, 18 mmol) and $Ti(OC_4H_9)_4$ (1.56 mL, 4.5 mmol) were added into a mixed solution of DMF and anhydrous CH_3OH (54 mL/6 mL). The mixture was stirred at room temperature for 30 min, and then transferred to a 100 mL Teflon autoclave and heated at 150 °C for 72 h. After cooling to ambient temperature, the solid was collected by centrifugation and washed with DMF and methanol for three times. Finally, the product was obtained by drying in a vacuum oven at 80 °C for 12 h.

Synthesis of C, N-TNS. For the preparation of C, N-TNS, NH_2-MIL-125 (0.16 g) and 8 mL DMF were put into 15 mL Teflon-lined autoclave, which was sonicated for 20 min and vigorously stirred for 20 min to obtain a suspension. The mixture was heated at 180 °C for 24 h. After cooling to room temperature, the solid was collected by centrifugation and washed by DMF and CH_3OH for three times. Finally, the product was obtained by drying in a vacuum oven at 25 °C for 12 h. Other samples were synthesized from NH_2-MIL-125 with different solvothermal treatment time through the same procedure.

Characterizations. X-ray diffraction (XRD) patterns were determined by a Rigaku D/max-2500 diffractometer equipped with Cu Kα radiation (λ = 1.5418 Å) at 40 kV and 200 mA. The morphologies of samples were observed on scanning electron microscopy (SEM, HITACHI SU-8020), transmission electron microscopy (TEM, JEOL

JEM-1011) and high-resolution TEM (HRTEM, JEOL-2100F) operated at 200 kV. The X-ray photoelectron spectra (XPS) were carried out with a multipurpose X-ray photoemission spectroscope (Thermo Scientific ESCALAB 250Xi). Fourier transform infrared (FT-IR) spectra were determined by a Bruker Tensor 27 spectrometer. The KBr pellet method was applied to prepare the solid samples. The optical absorption properties were characterized by ultraviolet visible diffused reflectance spectra (UV-Vis DRS, V-2600, SHIMADZU) using $BaSO_4$ as a reference for diffuse experiments. Photoluminescence (PL) spectra were recorded at room temperature with a Hitachi F-4600 fluorescence spectrophotometer with the excitation wavelength of 300 nm. The time-resolved fluorescent decay spectroscopy (TRFDS) measurements were performed on LifeSpec-II. The C and N contents of sample were measured by elemental analysis on FLASH EA1112 EA instrument. Electron spin resonance (ESR) spectra were collected on a Bruker ESP-300 spectrometer. The X-ray absorption find structure (XAFS) spectra for Ti K-edge were collected at 1W1B station in Beijing Synchrotron Radiation Facility (BSRF). The storage rings of BSRF were operated at 2.5 GeV with an average current of 250 mA. Using Si (111) double-crystal monochromator, the data collections were carried out in transmission mode using ionization chamber. All spectra were collected at ambient conditions. For XAFS analysis, the acquired EXAFS data were processed according to the standard procedures using ATHENA module implemented in IFEFFIT software packages. The k^3-weighted EXAFS spectra were obtained by subtracting the post-edge background from the overall absorption and normalizing with respect to the edge-jump step. Subsequently, k^3-weighted χ(k) data of Ti K-edge were Fourier transformed to real (R) space using hanning window (dk = 1.0 $Å^{-1}$) to separate the EXAFS contributions from different coordination shells. To obtain the quantitative structural parameters around central atoms, least-squares curve parameter fitting was performed using ARTEMIS module of IFEFFIT software packages.

Photocatalytic oxidation of thioanisole. In a typical experiment, 10 mg photocatalyst and 0.30 mmol of substrate were dispersed in 5 mL of acetonitrile in a 50 mL round-bottom flask and then vigorously stirred in air for 30 min to obtain a suspension. Then

the flask was plugged with a rubber stopper and irradiated by a 300 W Xe lamp (350 < λ < 780 nm, Aulight CEL-HX, Beijing). The reaction system was kept at 25 °C by a circulating water device. After the desired irradiation time, the liquid product was analyzed by ^{1}H nuclear magnetic resonance (^{1}H NMR, Bruker Avance III 400 HD). The conversion of thioanisole and selectivity to sulfoxide were calculated from the integration of ^{1}H NMR peaks using 1,3,5-trioxane as an internal standard. Control experiments without the addition of catalyst or light irradiation were conducted, respectively. No product was obtained, suggesting that the oxidation is motivated in the photocatalytic system. For the reusability study, the C, N-TNS catalyst after 5 h of reaction was recovered by centrifugation, washed with ethanol and dried under vacuum. Then the catalyst was added into 5 mL acetonitrile containing 0.30 mmol of thioanisole for a consecutive run.

Photocatalytic oxidation of benzylamine. In a typical experiment, 10 mg of photocatalyst and 0.20 mmol of benzylamine were dispersed in 5 mL of acetonitrile in a 50 mL round-bottom flask. The mixture was stirred in air for 30 min to obtain a suspension. The flask was plugged with a rubber stopper and irradiated by a 300 W Xe lamp (350 < λ < 780 nm, Aulight CEL-HX, Beijing). Then the reaction system was kept at 25 °C by a circulating water device. After the desired irradiation time, the liquid product was analyzed by ^{1}H NMR. The conversion of benzylamine and selectivity to *N*-benzylbenzaldimine were calculated from the integration of ^{1}H NMR peaks using 1,3,5-trioxane as an internal standard. Control experiments without the addition of catalyst or light irradiation were conducted, respectively. No product was obtained, suggesting that the oxidation was motivated in the photocatalytic system.

Photocatalytic oxidation of ethylbenzene. In a typical experiment, 10 mg of photocatalyst, 0.125 mmol of ethylbenzene and 0.2 equivalent of KBr were dispersed in 5 mL of methanol in a 50 mL round-bottom flask. The reaction mixture was stirred and irradiated by a 300 W Xe lamp (350 < λ < 780 nm, Aulight CEL-HX, Beijing) in O_2 atmosphere (1 atm). The reaction system was kept at 25 °C by a circulating water device. After the desired irradiation time, the liquid product was analyzed by ^{1}H NMR. The conversion of ethylbenzene and selectivity to acetophenone were calculated from

the integration of ^{1}H NMR peaks using 1,3,5-trioxane as an internal standard. Control experiments without the addition of catalyst or light irradiation were conducted, respectively. No product was obtained, suggesting that the oxidation was motivated in the photocatalytic system.

Quenching experiment. Quenching experiment was performed with the same procedure as photocatalytic oxidation of thioanisole, except the addition of 2 equivalent of scavengers (*p*-Benzoquinone (BQ) and beta-carotene).

ESR experiment. 2 mg of catalyst was dispersed in 2 mL of acetonitrile in a 50 mL round-bottom flask under dark condition. The mixture was stirred in air for 30 min to obtain a suspension. The suspension was mixed with 10 μL trapping agent of 2,2,6,6-tetramethylpiperidine (TEMP) or 5,5-dimethyl-1-pyrroline N-oxide (DMPO) in a 50 mL round-bottom flask. Then the mixture was light-illuminated for different time at room temperature and analyzed by Bruker ELEXSYS II E500.

Photoelectrochemical test. The photoelectrochemical measurement was implemented in a three-electrode system at electrochemical workstation (CHI660E, Chenhua Instrument, Shanghai, China) with the photocatalyst-coated indium-tin oxide (ITO) as the working electrode, an Ag/AgCl with 3.5 M KCl as a reference electrode and Pt net (1 cm^2) as the counter electrode. The illumination source adopted in photocurrent ON/OFF cycles was a 300 W Xe lamp ($350 < \lambda < 780$ nm). A 0.5 M Na_2SO_4 solution (pH = 6.8) was applied as electrolyte. To prepare the catalyst ink, 3 mg of the photocatalyst and 10 μL of 5 % Nafion 117 solution, as conducting binder, were introduced into 200 μL of ethanol and sonicated for 1 h. Then the catalyst ink was dropped on the surface of an ITO plate (1 cm^2) to prepare the working electrodes. Transient photocurrents, Mott-Schotty measurements and electrochemical impedance spectra (EIS) Nyquist plots were performed in 0.5 M Na_2SO_4 solution. All the potentials were recorded versus Ag/AgCl (*vs.* Ag/AgCl) electrode.

2. Results and Discussion

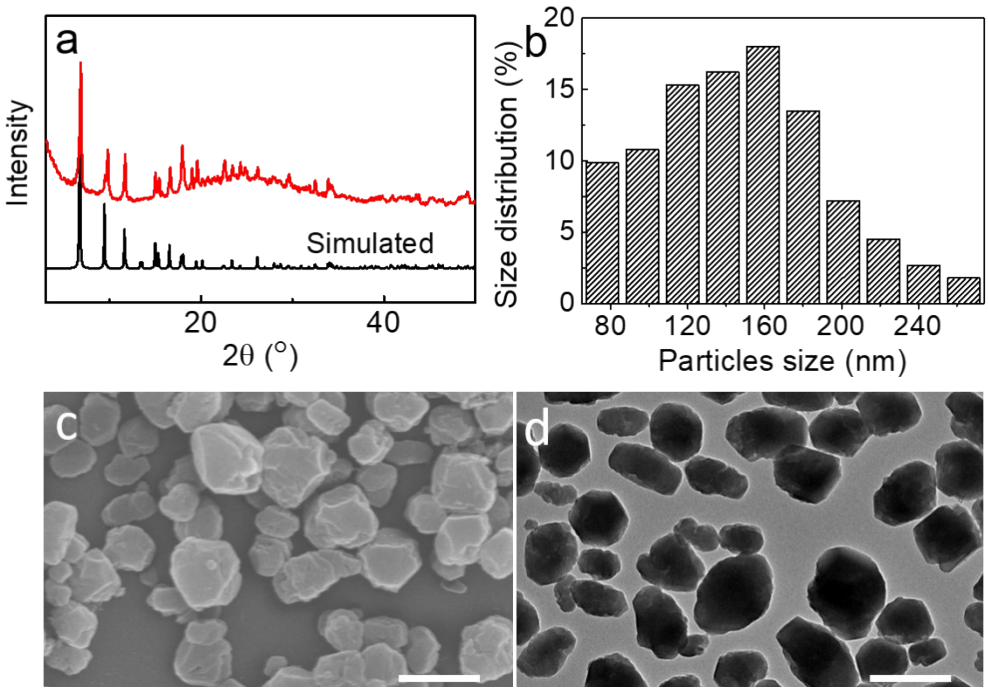

Fig. S1. XRD patterns (a), particle size distribution (b), SEM (c) and TEM (d) images of NH_2-MIL-125. Scale bars: 400 nm in (c) and 300 nm in (d).

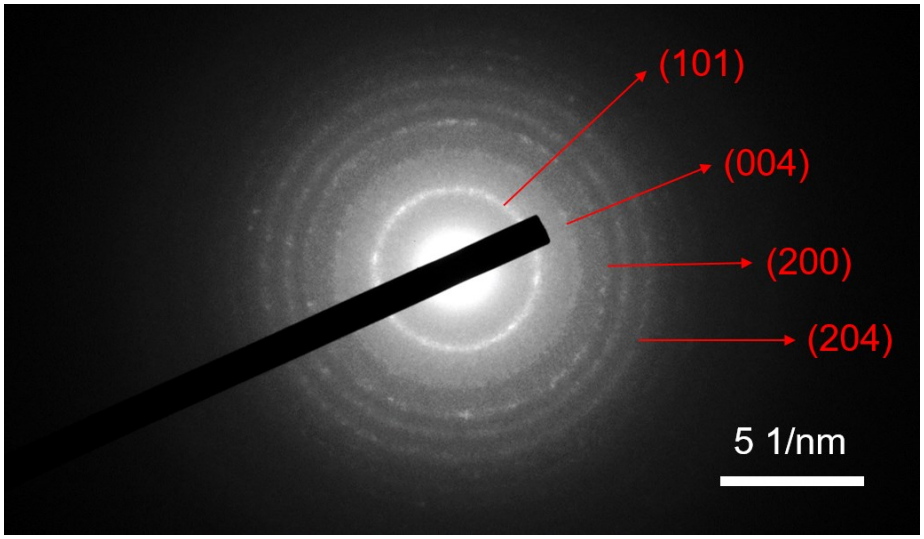

Fig. S2. SAED pattern of C, N-TNS.

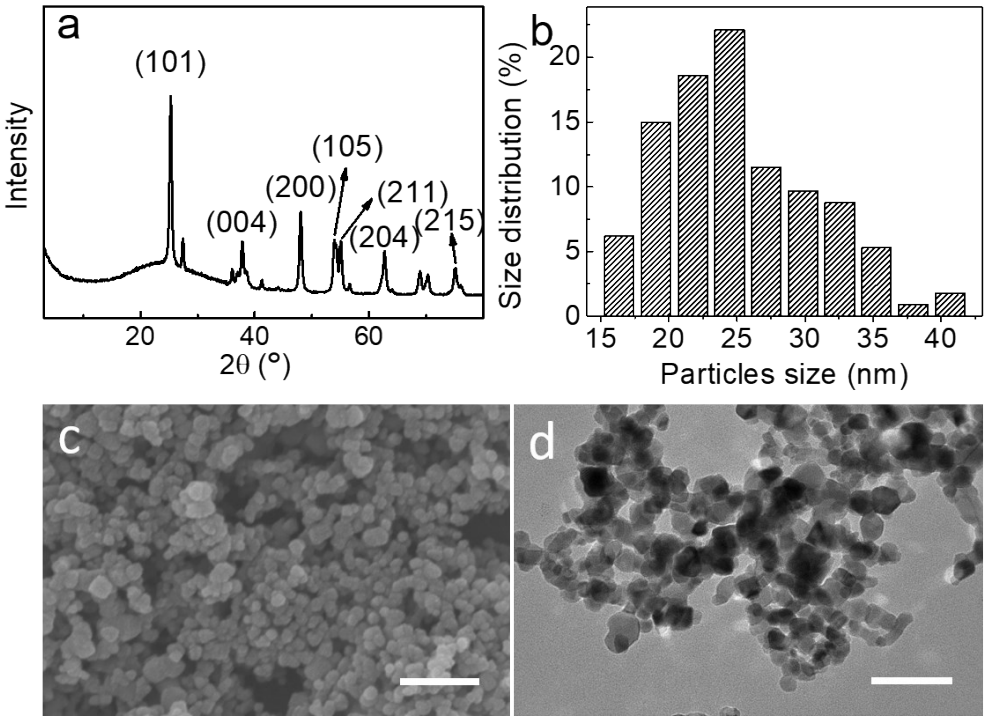

Fig. S3. XRD pattern (a), particle size distribution (b), SEM (c) and TEM (d) images of P25. Scale bars: 200 nm in (c) and 100 nm in (d).

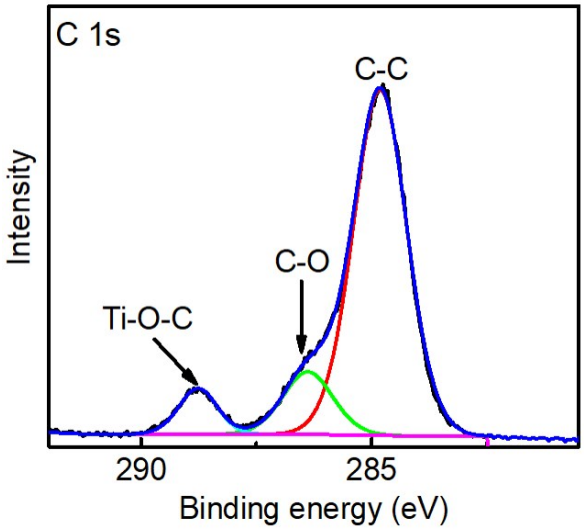

Fig. S4.. XPS spectra of C 1s of C, N-TNS. For the high-resolution C 1s XPS spectrum of C, N-TNS, the binding energies of 284.8 and 286.4 eV represent C-C and C-O species, respectively. The peak value of 288.8 eV is assigned to the partial substitution of C for the lattice titanium atoms to form Ti-O-C bonds in C, N-TNS. The appearance of Ti-O-C bonds indicates the formation of carbonate species. The peak at around 281.0 eV of Ti-C bond was not observed, which suggests that the carbon was incorporated into TiO_2 as carbonate species rather than substituting oxygen atom in the lattice of TiO_2.[1]

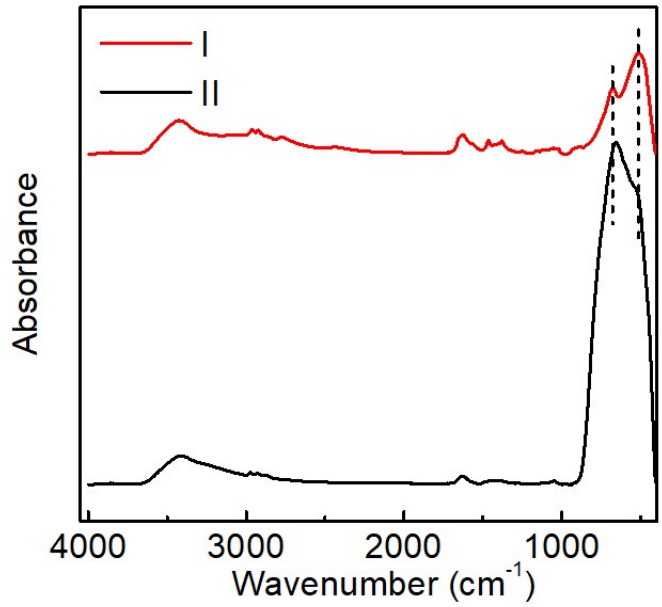

Fig. S5. FT-IR spectra of C, N-TNS (I) and P25 (II). The broad absorptions between 400 and 850 cm^{-1} are related to the stretching vibration of Ti-O and bridging stretching mode of Ti-O-Ti corresponding to TiO_2.[2] The Ti-O-Ti stretching peak of C, N-TNS is slightly shifted to lower wavenumber (507 cm^{-1}) compared with P25 (526 cm^{-1}), which results from the formation of oxygen vacancies.[3] Remarkably, the absorption peak position of Ti-O at 679 cm^{-1} of C, N-TNS is higher than that of P25 (656 cm^{-1}). It can be ascribed to the formation of N-Ti-O bonds.[4] Furthermore, the broad peak intensity (400-850 cm^{-1}) of C, N-TNS decreases obviously compared with that of P25, corresponding to the presence of Ti-O-C bending vibrations.[5]

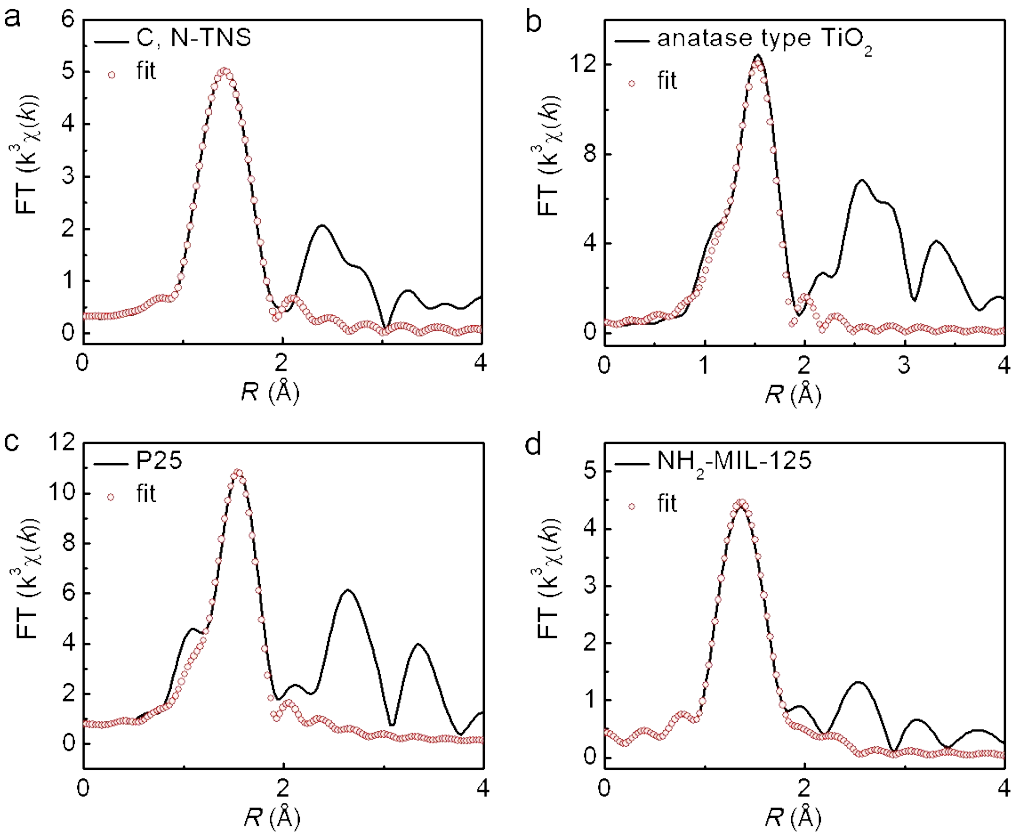

Fig. S6. EXAFS fitting curves of C, N-TNS (a), anatase type TiO_2 (b), P25 (c) and NH_2-MIL-125 (d) in *R* space.

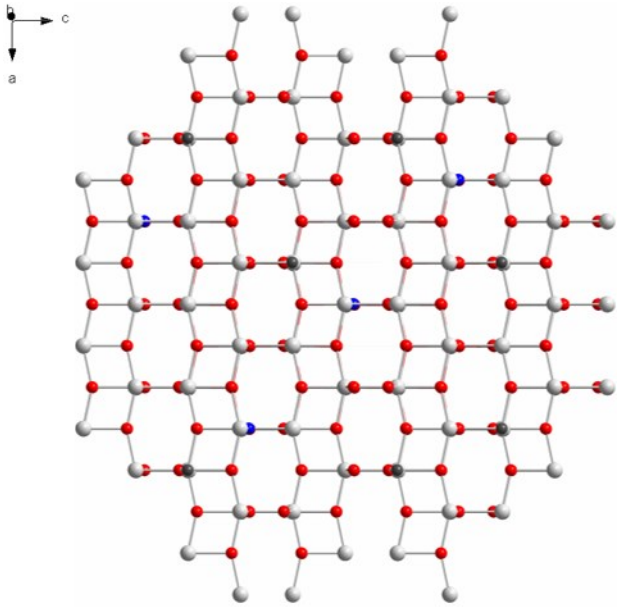

Fig. S7. Schematic model of C, N-TNS: Ti (light gray), N (blue), C (dark gray) and O (red).

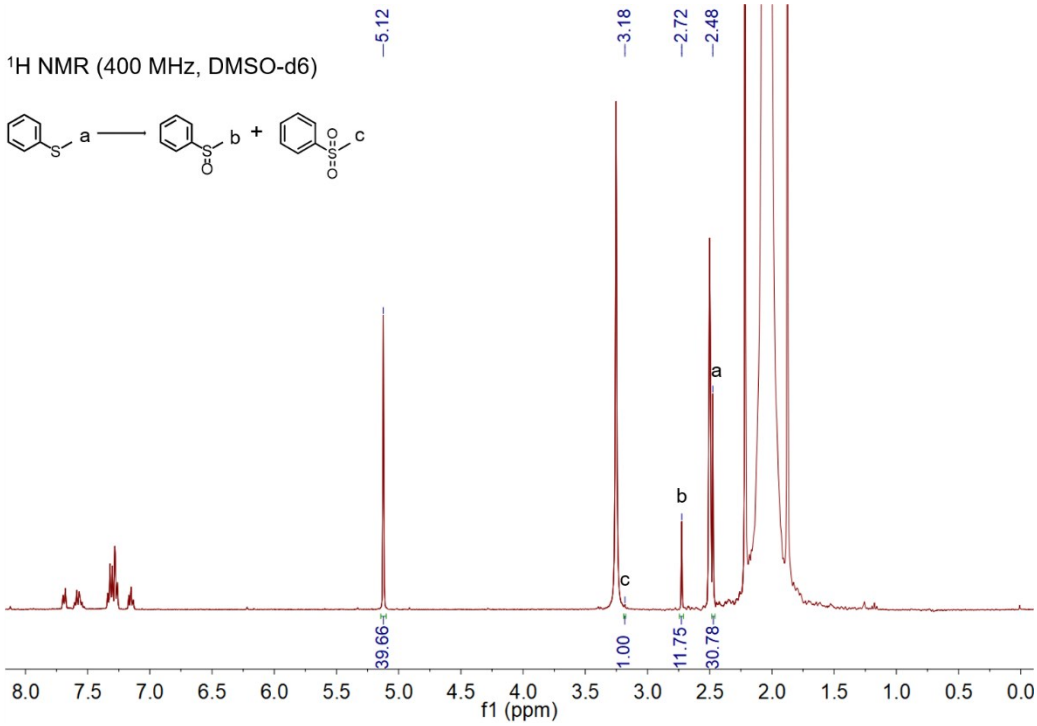

Fig. S8. ^{1}H NMR spectrum for the oxidations of thioanisole catalyzed by P25 at 6 h. The characteristic peak of 1,3,5-trioxane (internal standard) is at 5.12 ppm in DMSO-d6.

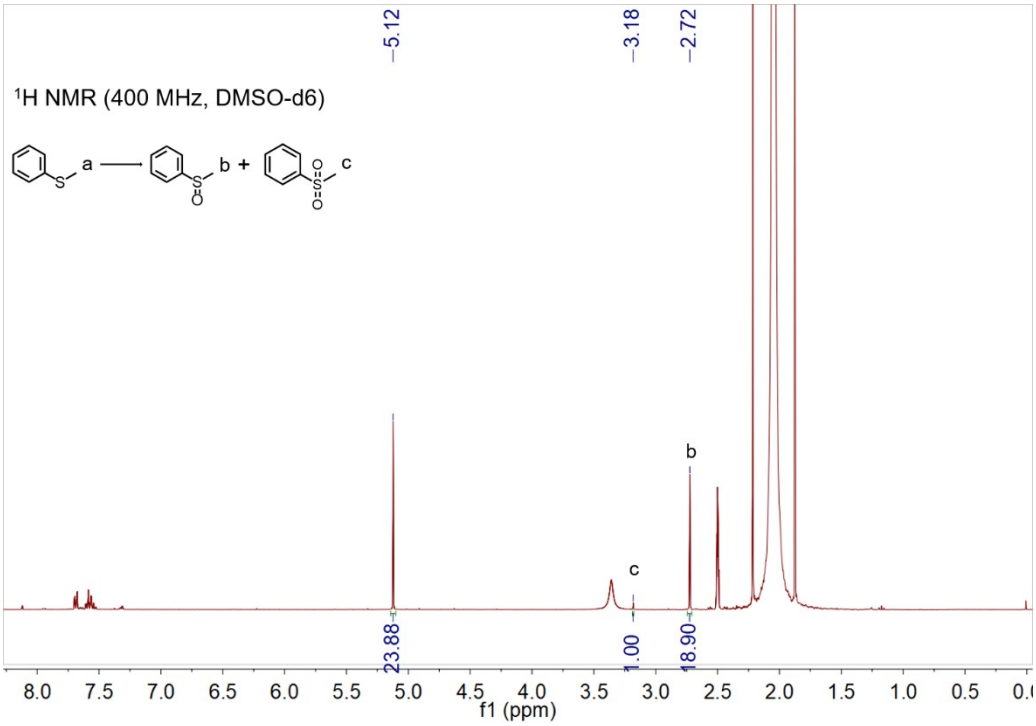
¹H NMR (400 MHz, DMSO-d6)
a
b +
c
5.12
3.18
2.72
b
c
23.88
1.00
18.90
f1 (ppm)

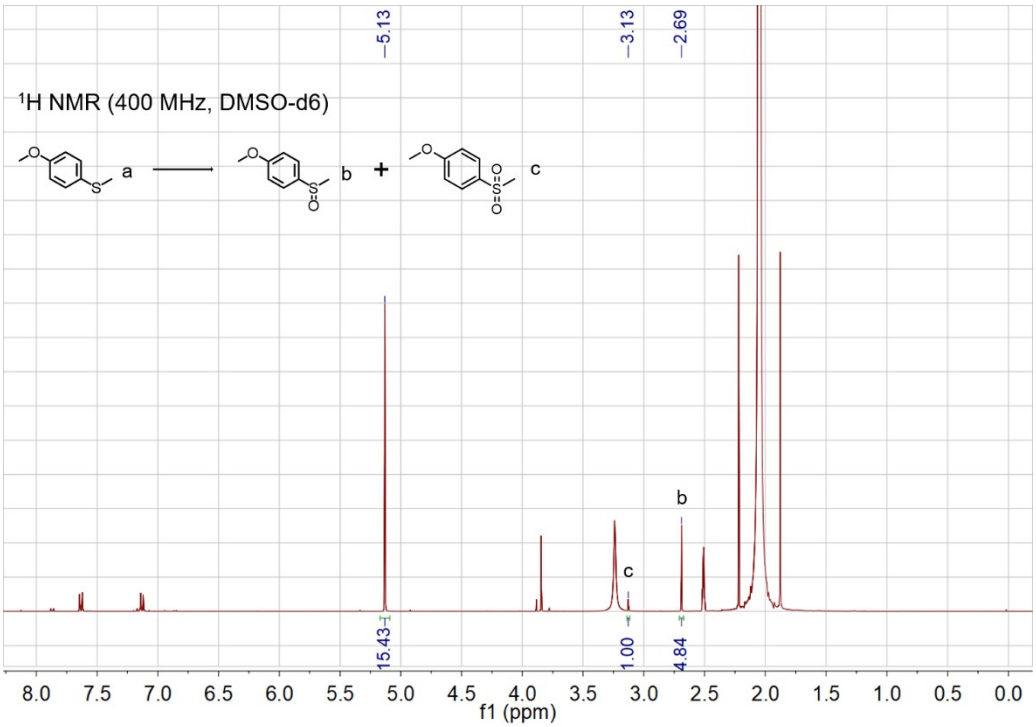
¹H NMR (400 MHz, DMSO-d6)
a
b
+
c
5.13
3.13
2.69
b
c
15.43
1.00
4.84
f1 (ppm)

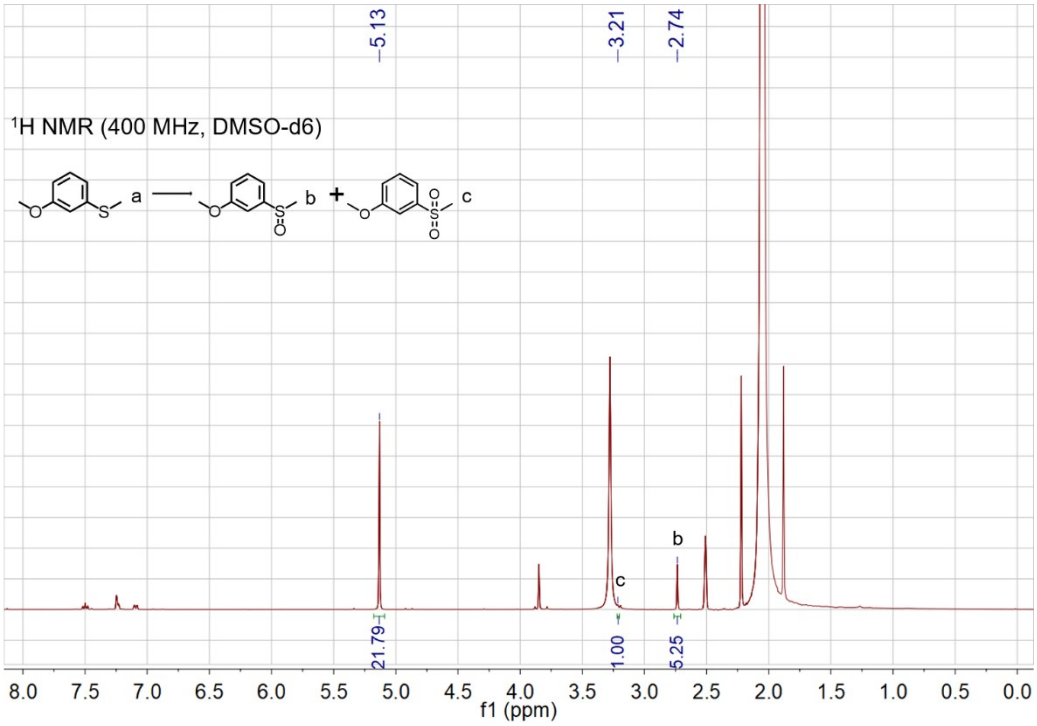
5.13
3.21
2.74
¹H NMR (400 MHz, DMSO-d6)
a
b
c
21.79
1.00
5.25
8.0 7.5 7.0 6.5 6.0 5.5 5.0 4.5 4.0 3.5 3.0 2.5 2.0 1.5 1.0 0.5 0.0
f1 (ppm)

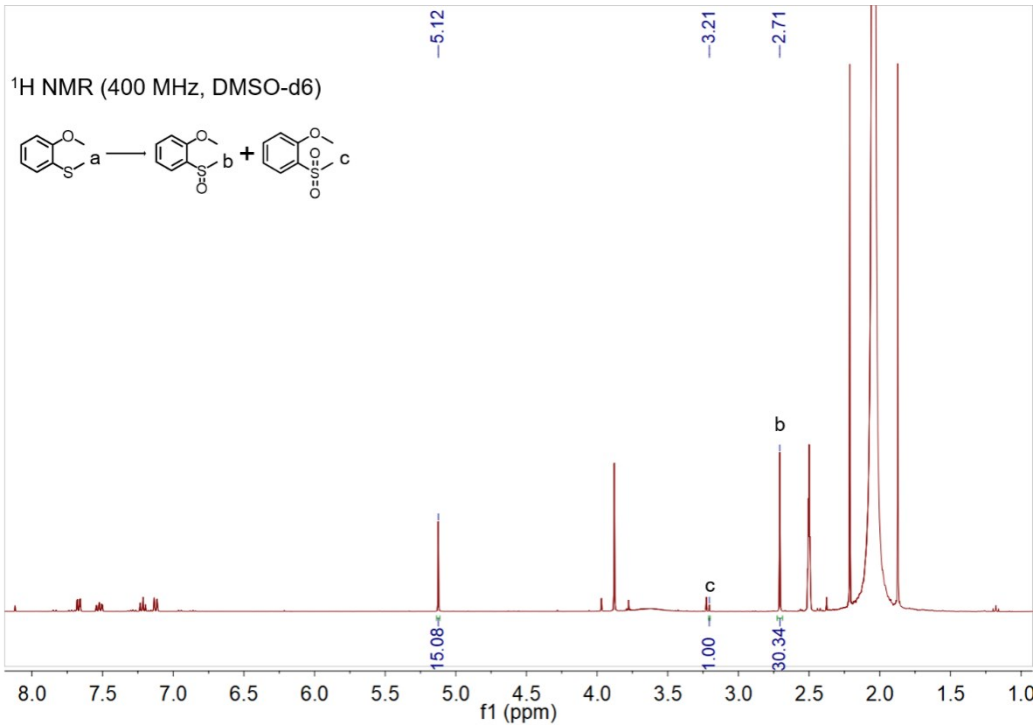
5.12
3.21
2.71
¹H NMR (400 MHz, DMSO-d6)
a
b
c
15.08
1.00
30.34
8.0 7.5 7.0 6.5 6.0 5.5 5.0 4.5 4.0 3.5 3.0 2.5 2.0 1.5 1.0
f1 (ppm)

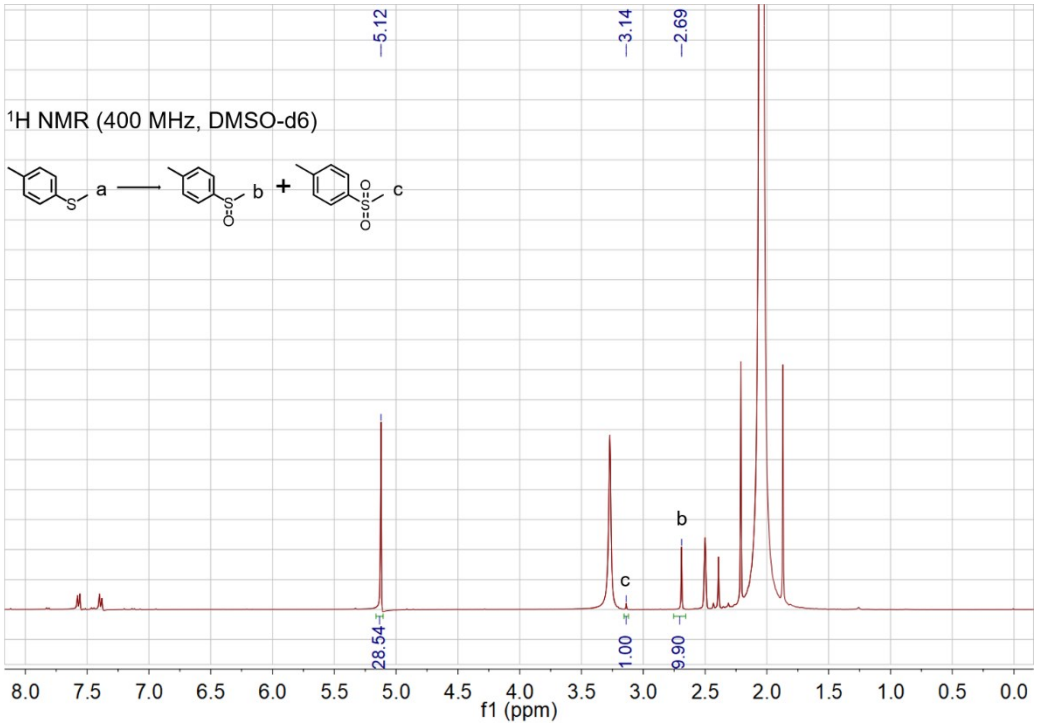
5.12
3.14
2.69
1H NMR (400 MHz, DMSO-d6)
a
b
c
28.54
1.00
9.90
f1 (ppm)

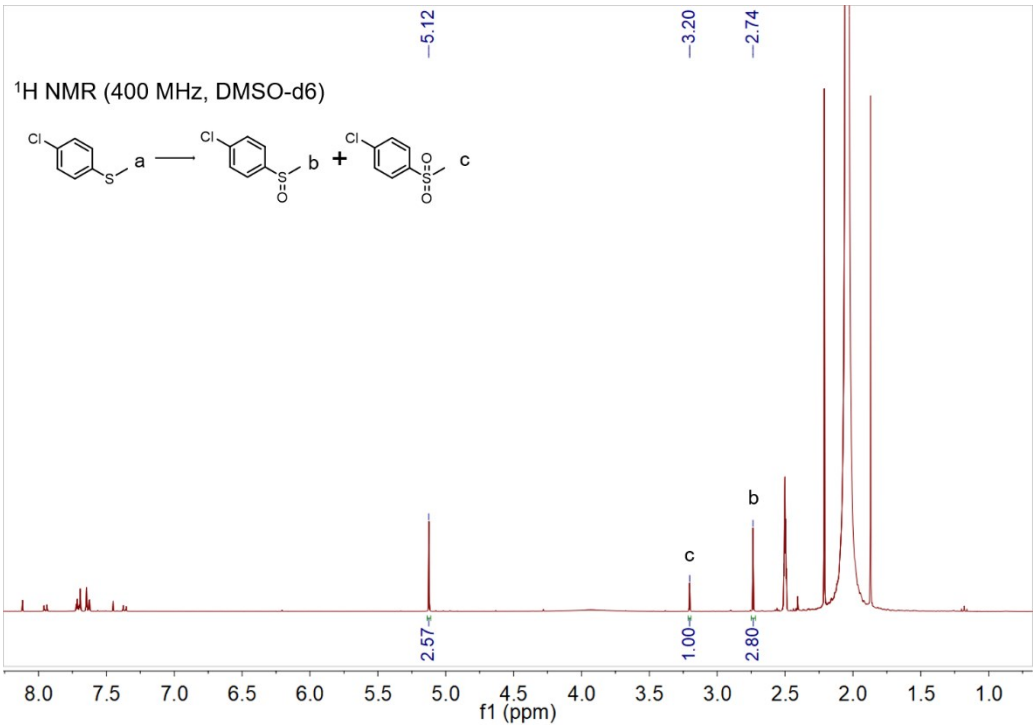
5.12
3.20
2.74
1H NMR (400 MHz, DMSO-d6)
Cl
a
b
c
2.57
1.00
2.80
f1 (ppm)

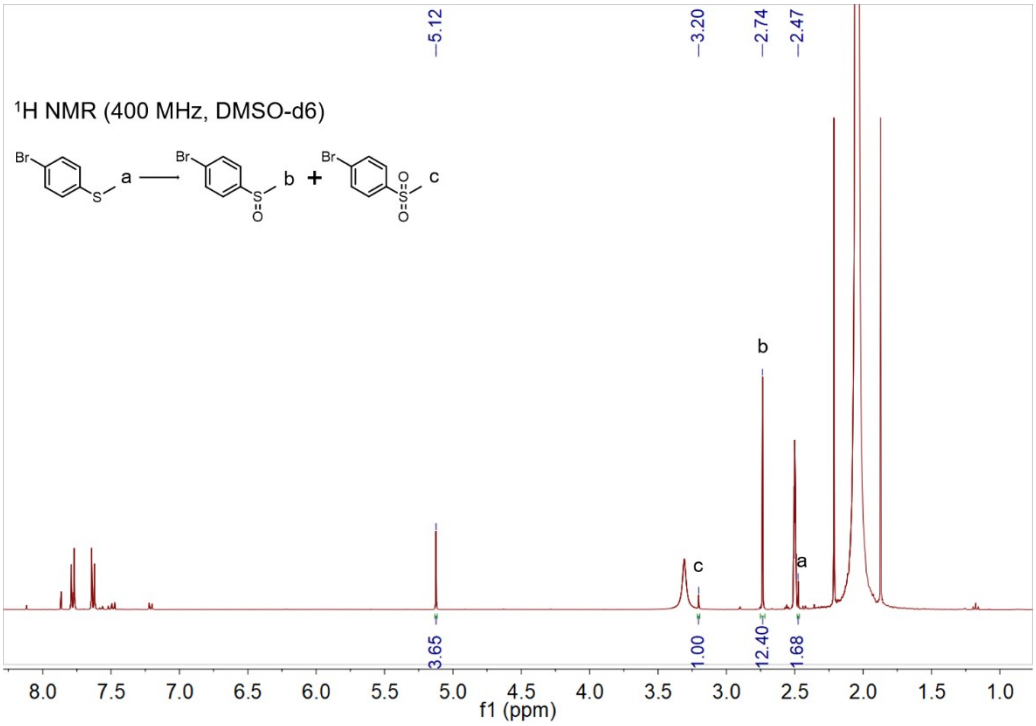
5.12
3.20
2.74
2.47
¹H NMR (400 MHz, DMSO-d6)
Br
a
b
c
b
c
a
3.65
1.00
12.40
1.68
8.0 7.5 7.0 6.5 6.0 5.5 5.0 4.5 4.0 3.5 3.0 2.5 2.0 1.5 1.0
f1 (ppm)

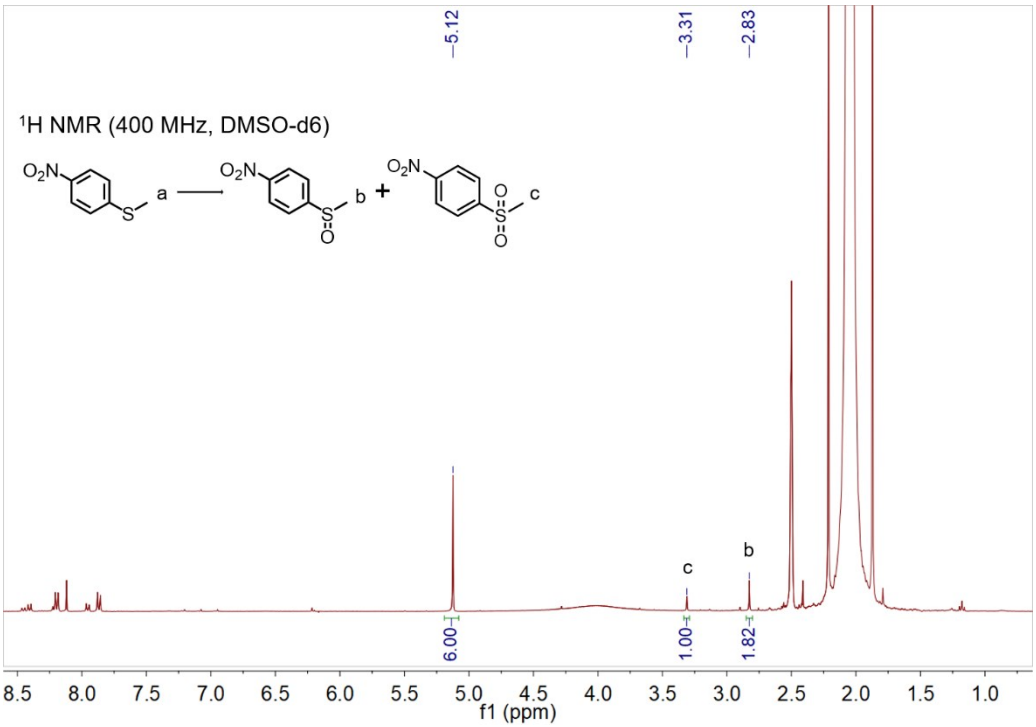
5.12
3.31
2.83
¹H NMR (400 MHz, DMSO-d6)
O2N
a
b
c
c
b
6.00
1.00
1.82
8.5 8.0 7.5 7.0 6.5 6.0 5.5 5.0 4.5 4.0 3.5 3.0 2.5 2.0 1.5 1.0
f1 (ppm)

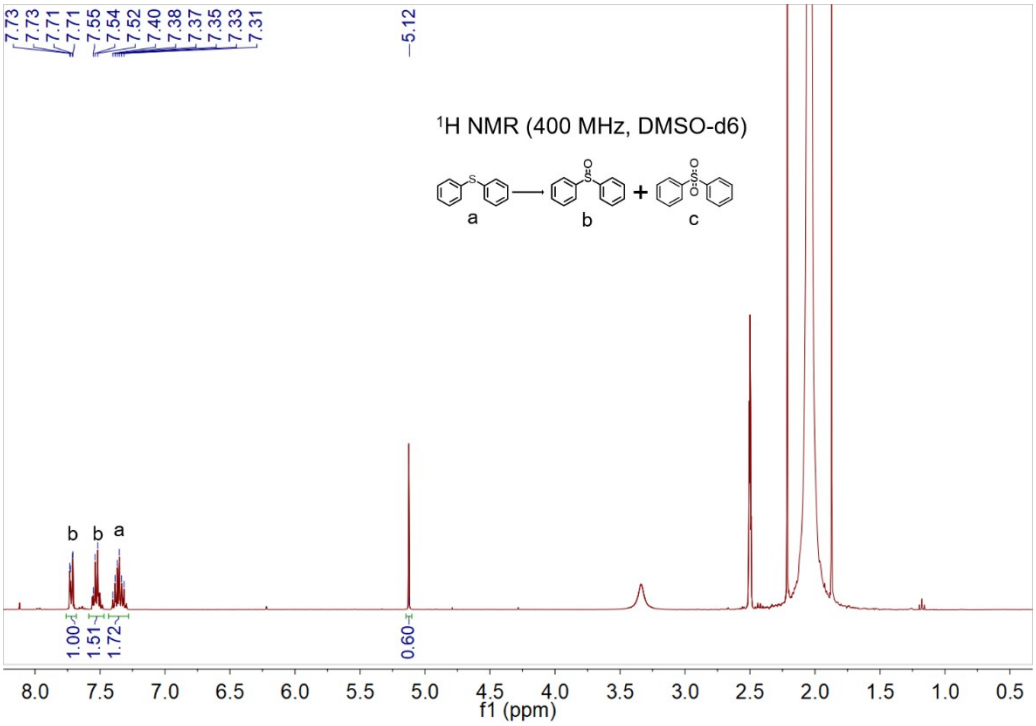
7.73
7.73
7.71
7.71
7.55
7.54
7.52
7.40
7.38
7.37
7.35
7.33
7.31
5.12
¹H NMR (400 MHz, DMSO-d6)
a
b
c
b b a
1.00
1.51
1.72
0.60
8.0 7.5 7.0 6.5 6.0 5.5 5.0 4.5 4.0 3.5 3.0 2.5 2.0 1.5 1.0 0.5
f1 (ppm)

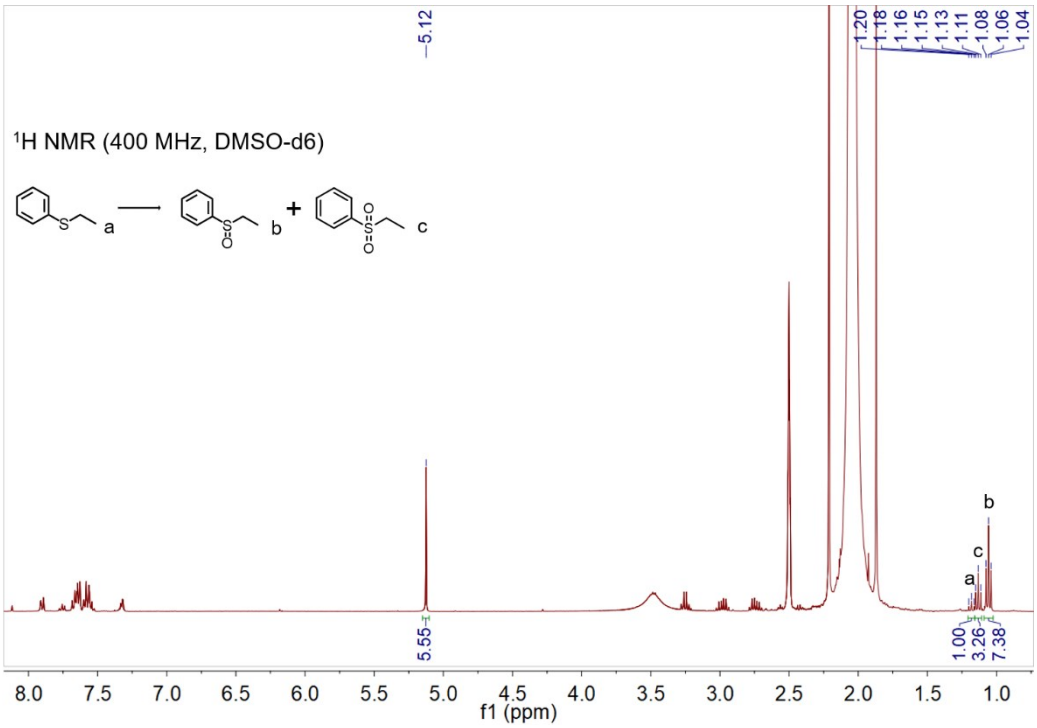
5.12
1.20
1.18
1.16
1.15
1.13
1.11
1.08
1.06
1.04
¹H NMR (400 MHz, DMSO-d6)
a
b
c
b
c
a
5.55
1.00
3.26
7.38
8.0 7.5 7.0 6.5 6.0 5.5 5.0 4.5 4.0 3.5 3.0 2.5 2.0 1.5 1.0
f1 (ppm)

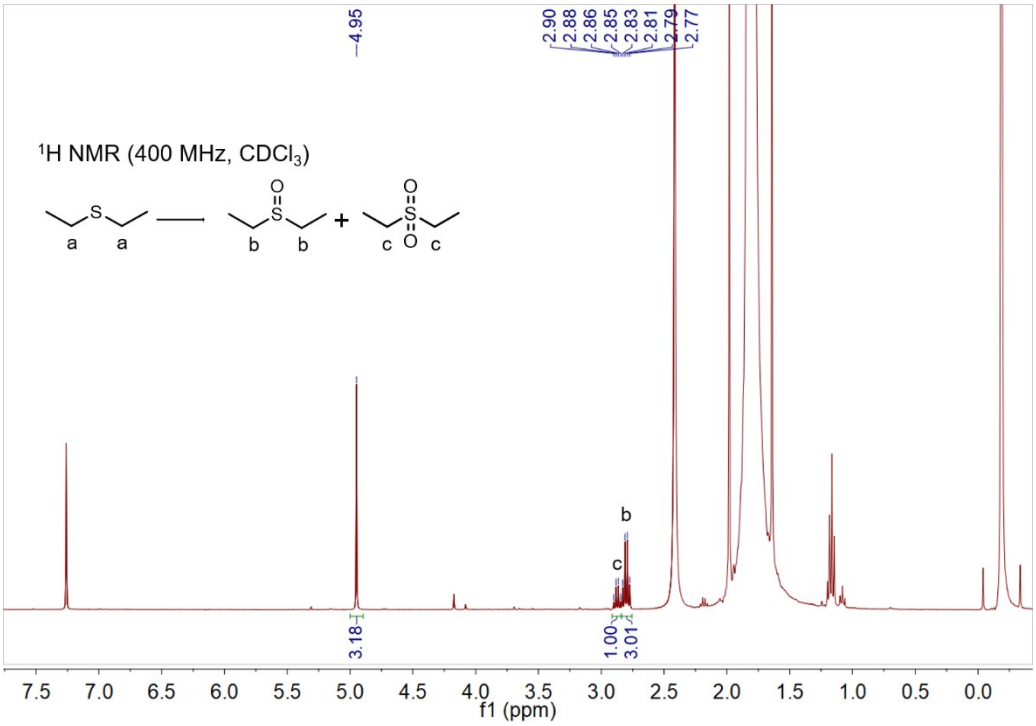
1H NMR (400 MHz, CDCl3)
4.95
2.90
2.88
2.86
2.85
2.83
2.81
2.79
2.77
a
a
b
b
c
c
O
b
c
3.18
1.00
3.01
7.5 7.0 6.5 6.0 5.5 5.0 4.5 4.0 3.5 3.0 2.5 2.0 1.5 1.0 0.5 0.0
f1 (ppm)

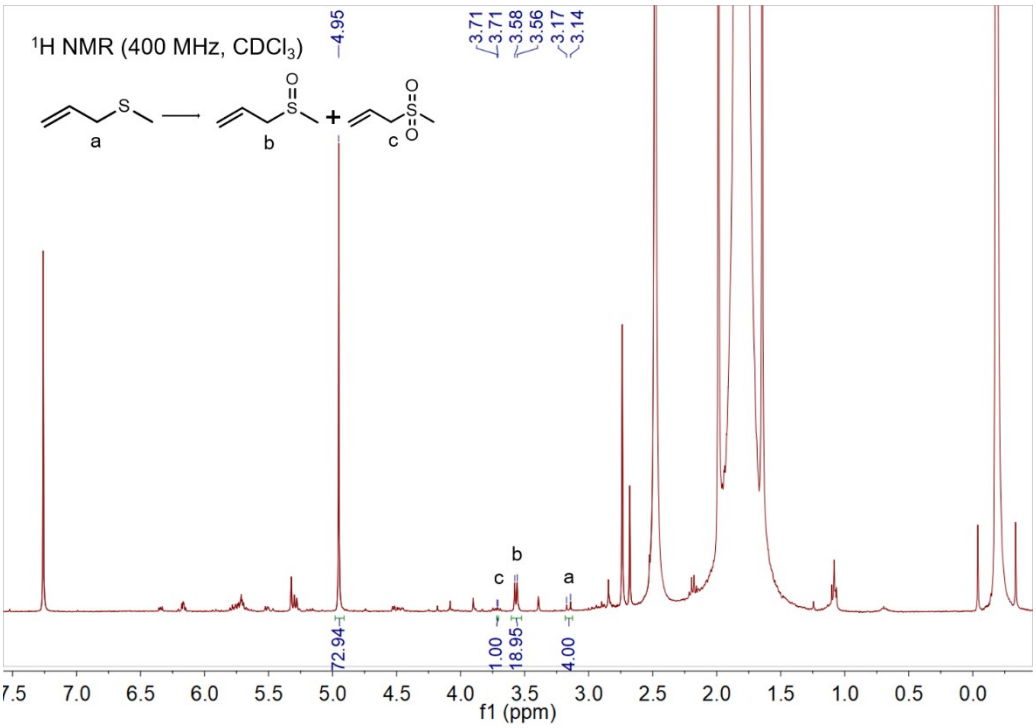
1H NMR (400 MHz, CDCl3)
4.95
3.71
3.71
3.58
3.56
3.17
3.14
a
b
c
O
b
c
a
72.94
1.00
18.95
4.00
7.5 7.0 6.5 6.0 5.5 5.0 4.5 4.0 3.5 3.0 2.5 2.0 1.5 1.0 0.5 0.0
f1 (ppm)

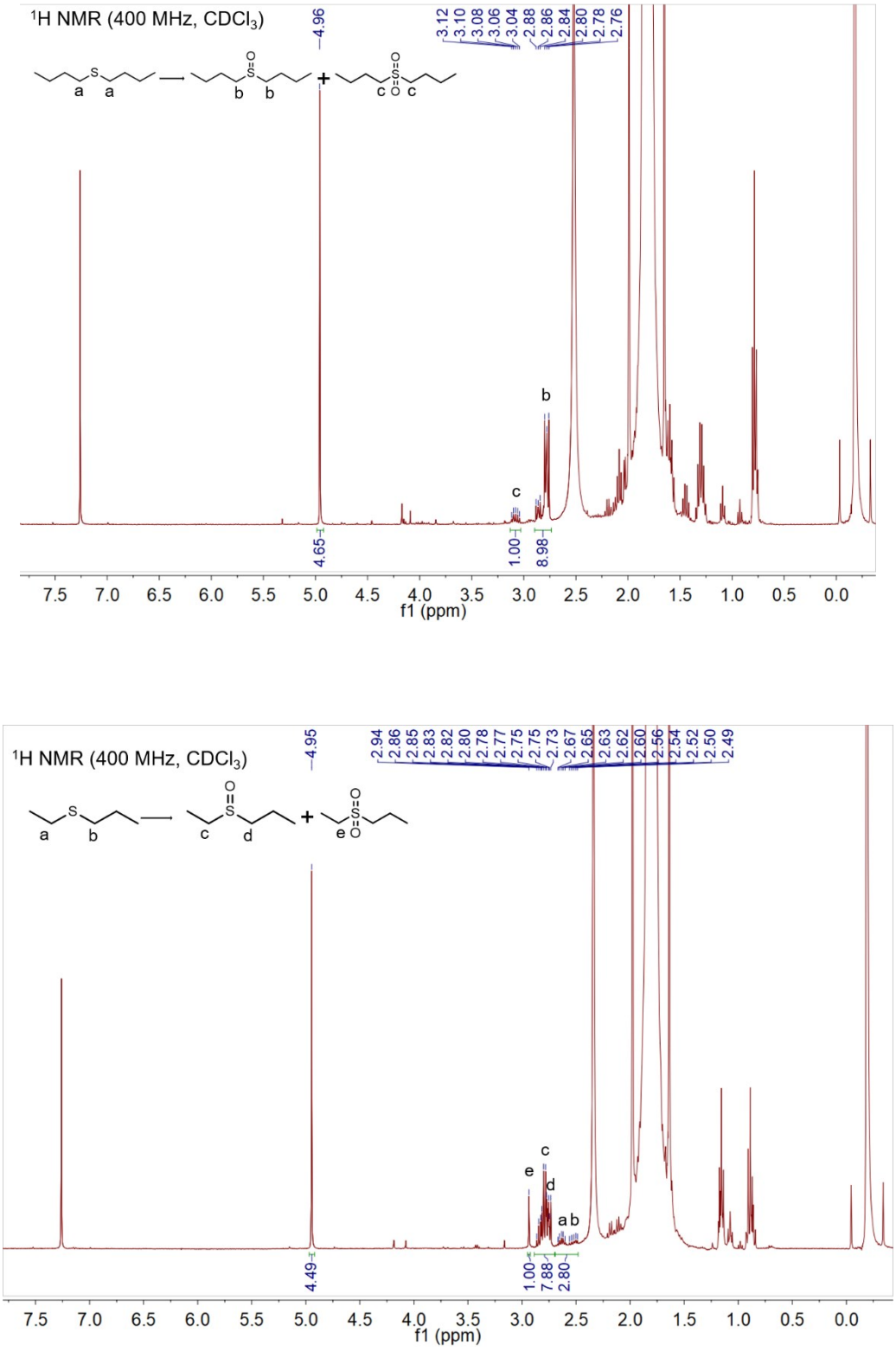

Fig. S9. ¹H NMR spectra for the oxidations of various sulfides derivatives catalyzed by C, N-TNS at 6 h. The characteristic peak of 1,3,5-trioxane (internal standard) is at about 5.12 ppm in DMSO-d6 or 4.95 ppm in $CDCl_3$.

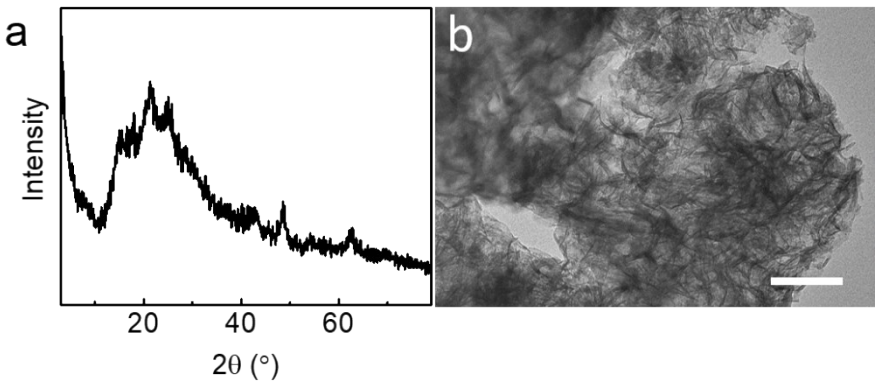

Fig. S10. XRD pattern (a) and TEM image (b) of C, N-TNS after 5 catalysis runs. Scale bar: 150 nm.

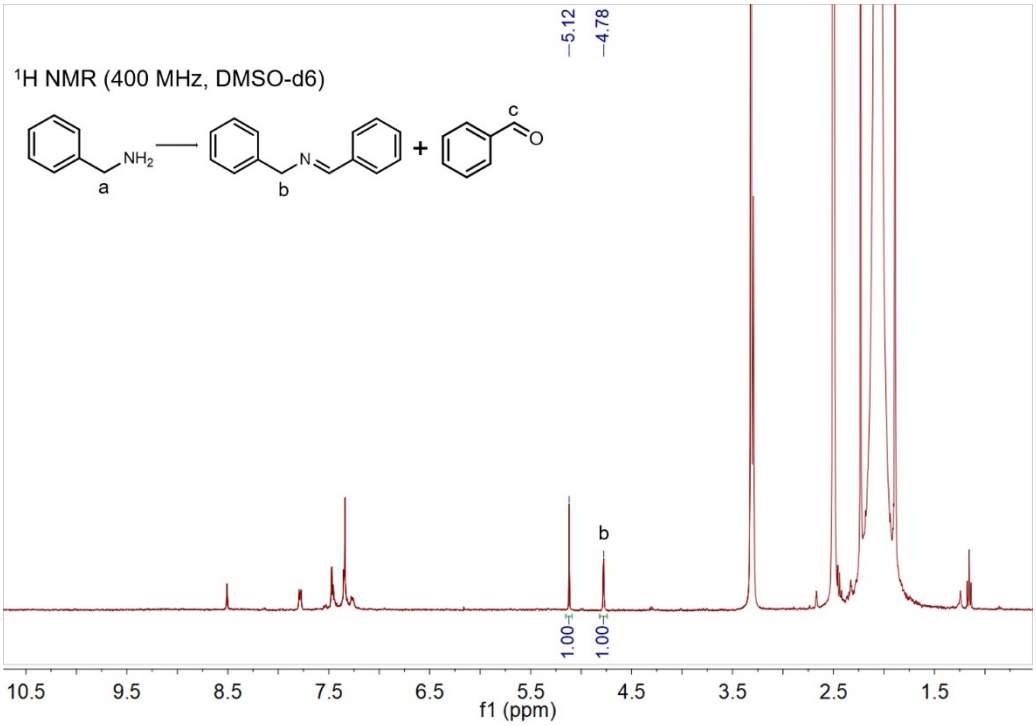

Fig. S11. ^{1}H NMR spectrum for the photocatalytic oxidation of benzylamine to *N*-benzylbenzaldimine catalyzed by C, N-TNS at 3 h. The characteristic peak of 1,3,5-trioxane (internal standard) is at 5.12 ppm in DMSO-d6.

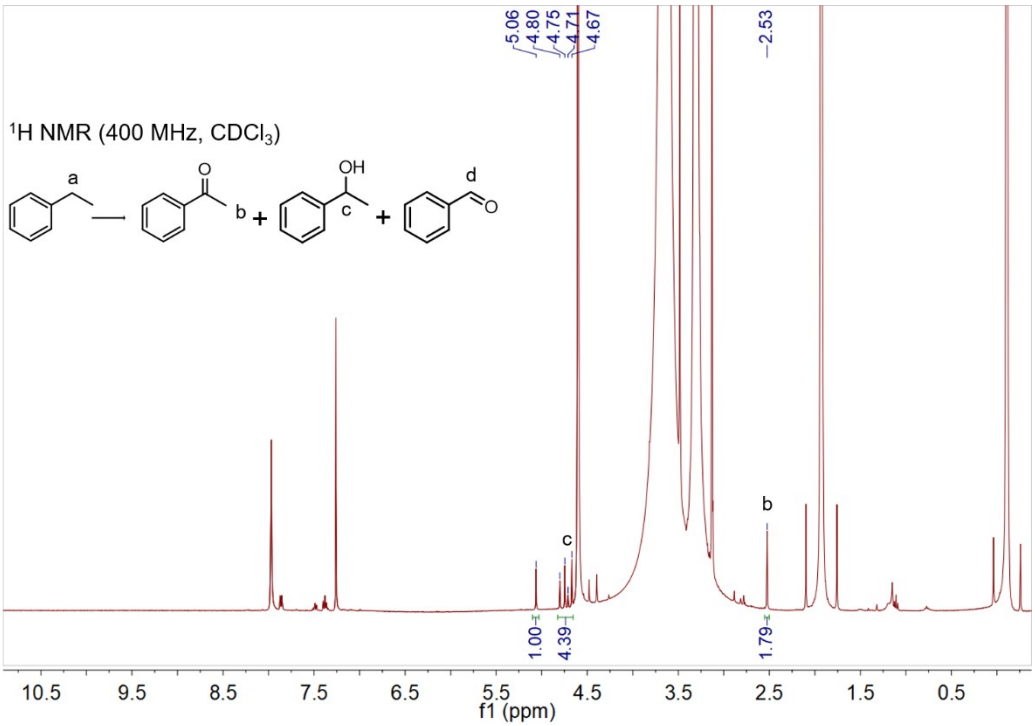

Fig. S12. ^{1}H NMR spectrum for the photocatalytic selective oxidation of ethylbenzene catalyzed by C, N-TNS at 24 h. The characteristic peak of 1,3,5-trioxane (internal standard) is at 5.06 ppm in $CDCl_3$.

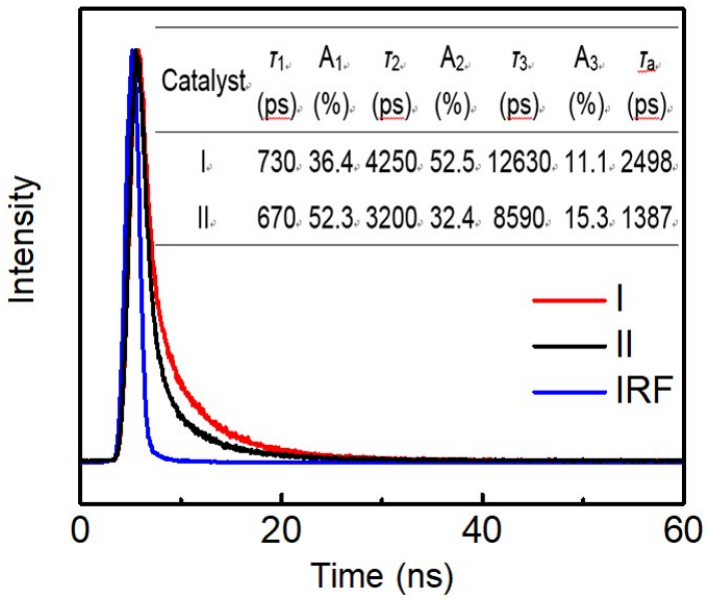

Fig. S13. TRFDS spectra of C, N-TNS (I) and P25 (II).

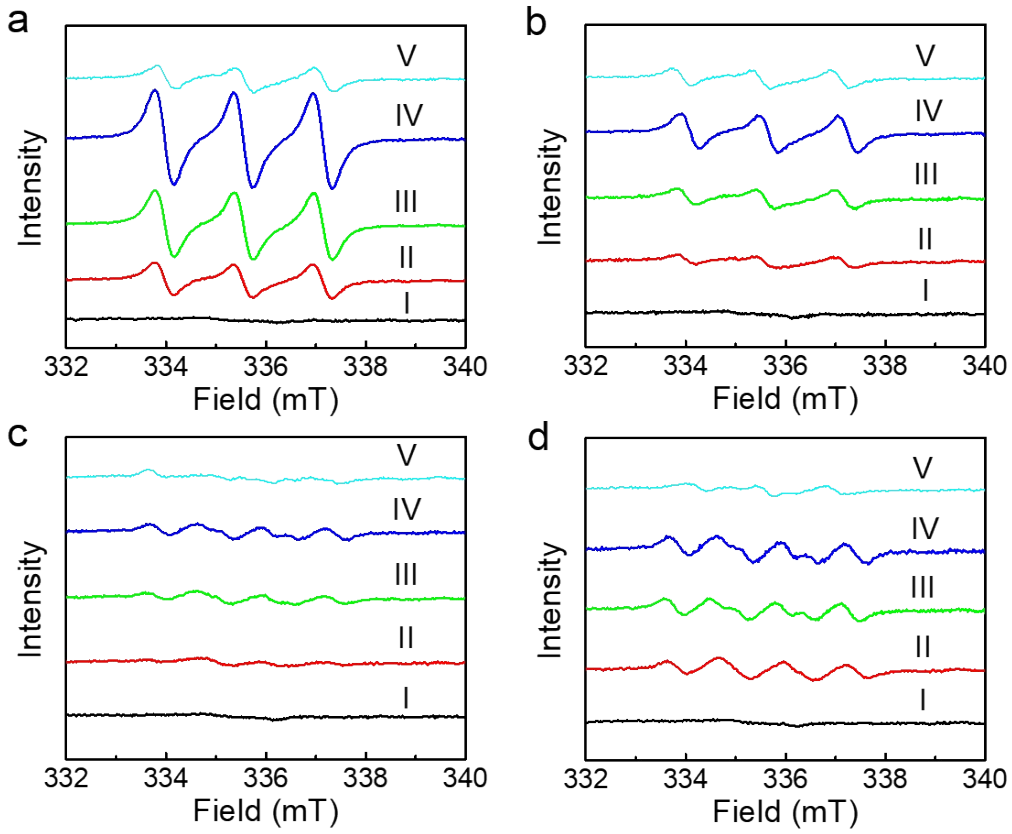

Fig. S14. (a, b) ESR spectra of C, N-TNS (a) and P25 (b) in the presence of TEMP. (c, d) ESR spectra of C, N-TNS (c) and P25 (d) in the presence of DMPO. Curve I: without thioanisole and in the dark. Curves II-IV: without thioanisole and under illumination for 15 s (II), 60 s (III) and 120 s (IV), respectively. Curve V: with thioanisole and under illumination for 720 s.

In the dark, no characteristic ESR signals were detected. After irradiation, there are characteristic signals of the DMPO-$O_2^{\bullet-}$ and TEMP-$^1O_2$ adducts. Notably, the intensities of ESR responses enhance with the increase of illumination time, confirming the formation of $O_2^{\bullet-}$ and $^1O_2$ by light irradiation. As shown in Fig. S14a, the 1:1:1 triplet signal of 2,2,6,6-tetramethylpiperidine-1-oxyl (TEMPO) is largely enhanced with the increased illumination time in the presence of C, N-TNS, indicating more $^1O_2$ is produced in the photocatalytic oxidation process. In a sharp contrast, the signal of P25 is greatly suppressed (Fig. S14b), suggesting much less $^1O_2$ yield in photocatalytic oxidation process. Moreover, the C, N-TNS system with DMPO shows the ESR spectra with negligible signals for DMPO-$O_2^{\bullet-}$ (Fig. S14c), corresponding to the little generation

of $O_2^{\bullet-}$. However, the P25 system produces considerable $O_2^{\bullet-}$ in O_2 activation through the charge-transfer process (Fig. S14d), which competes with the energy-transfer process related $^1O_2$ generation. These results suggest that $^1O_2$ is key ROS for the photocatalytic oxidation of sulfides. Then thioanisole was added to the reaction system to recognize the reactivity of sulfides with ROS. The ESR signals are obviously decreased with elongated reaction time, demonstrating that $O_2^{\bullet-}$ and $^1O_2$ species interact with thioanisole. All these data indicate that $^1O_2$ is the predominant ROS in the photocatalytic oxidation process.

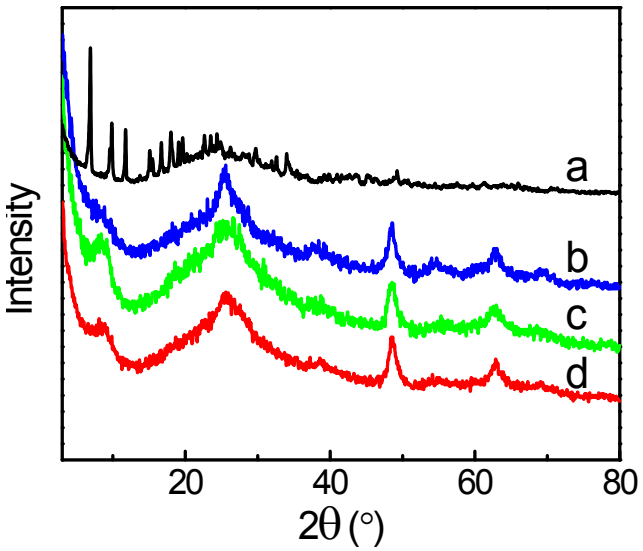

Fig. S15. XRD patterns of various products synthesized from NH_2-MIL-125 with solvothermal treatment time of 2 h (a), 6 h (b), 12 h (c) and 18 h (d).

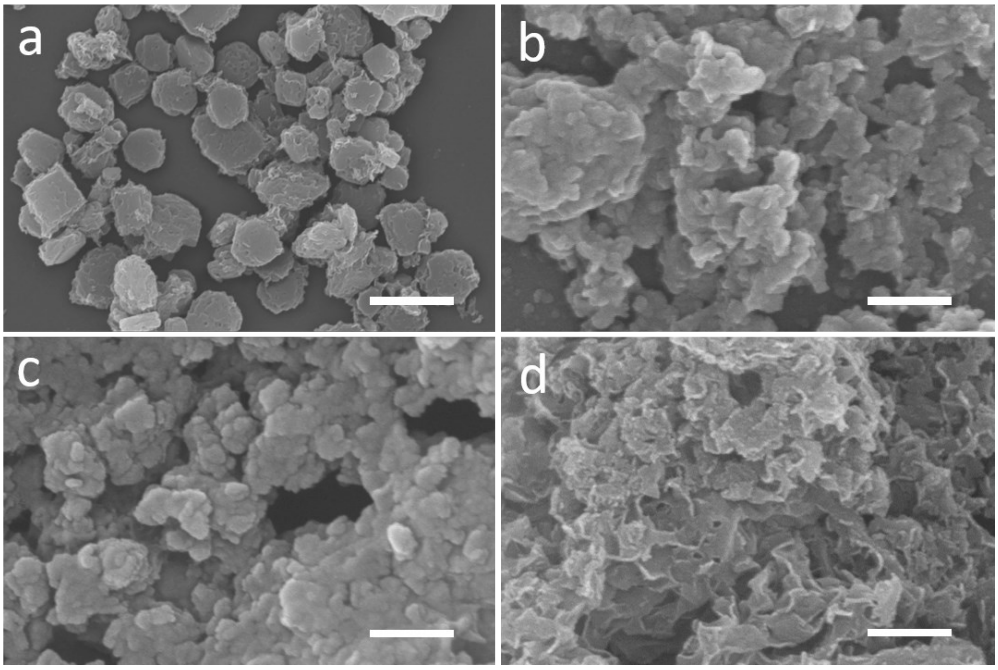

Fig. S16. SEM images of various products synthesized from NH_2-MIL-125 with solvothermal treatment time of 2 h (a), 6 h (b), 12 h (c) and 18 h (d). Scale bars: 1 um in (a) and 200 nm in (b-d).

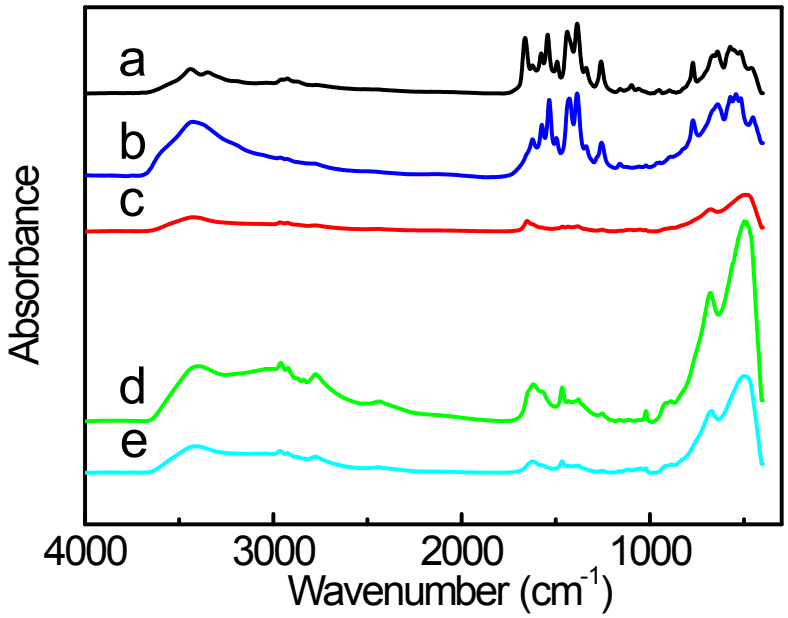

Fig. S17. FT-IR spectra of NH_2-MIL-125 (a) and its derivatives obtained at solvothermal treatment time of 2 h (b), 6 h (c), 12 h (d) and 18 h (e). FT-IR spectrum of NH_2-MIL-125 shows asymmetric (1578 and 1543 cm^{-1}) and symmetric (1439 and 1387 cm^{-1}) stretching vibrations for C=O in carboxylic groups.[6] All these groups are gradually decreased with prolonged time, indicating the loss of organic linkers from NH_2-MIL-125.

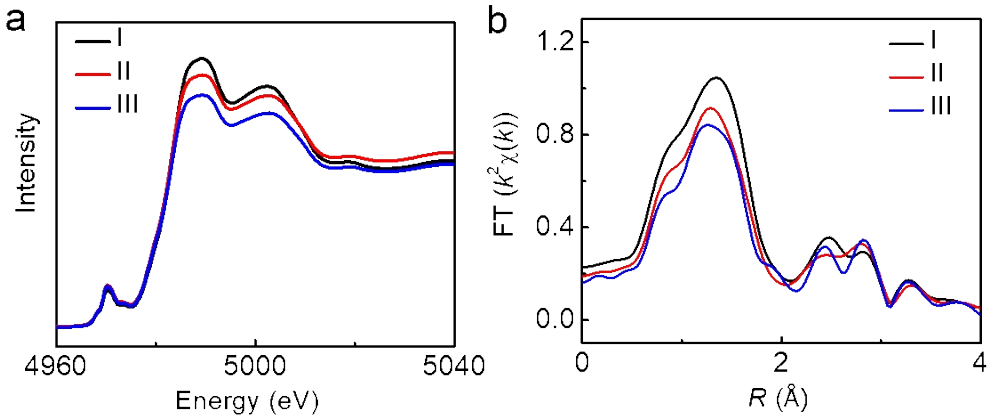

Fig. S18. Ti K-edge XANES spectra (a) and k^3-weighted χ(k) function of the EXAFS spectra (b) of C, N-TNS products synthesized from NH_2-MIL-125 with solvothermal treatment time of 6 h (I), 12 h (II) and 18 h (III). RDFs obtained from k^3-weighted χ(k) function of the EXAFS data indicate that the signal intensity of Ti-O bond gradually decreases with prolonged time, indicating the more loss of Ti-O bond.

Table S1. Ti K-edge EXAFS curve-fitting parameters of C, N-TNS and reference samples.[a]

Samples	Shell	N[b]	R (Å)[c]	ΔE_0 (eV)[d]	δ^2 (Å^2)[e]	R-factor[f]
C, N-TNS	Ti-O	4.1	1.92	3.1	0.0103	0.002
NH_2-MIL-125	Ti-O	4.4	1.89	-0.9	0.0130	0.006
P25	Ti-O	3.8	1.92	7.7	0.0020	0.009
	Ti-O	2.2	2.04		0.0025	
anatase type TiO_2	Ti-O	4	1.94	2.0	0.0056	0.007
	Ti-O	2	1.97		0.0050	

[a] k^3-weighted EXAFS. [b] N: average coordination numbers. [c] R: average interatomic distance. [d] ΔE_0: edge-energy shift. [e] δ^2: Debye-Waller factor. [f] R-factor: goodness of fit.

The amplitude reduction factor (S_0^2) was set as 0.784 for Ti-O, which was obtained from the experimental EXAFS fit of reference anatase type TiO_2 by fixing N as the known crystallographic value and was fixed to all the samples. The fits of a series of catalysts were performed in k-space (Δk) and R space (ΔR) are 2.00-10.70 Å^{-1} and 1.00-2.00 Å, respectively. Error bounds that characterize the structural parameters obtained by EXAFS spectra were estimated as N ± 20%; R ± 0.03 Å; δ^2 ± 20%.

Table S2. Comparison of the reaction conditions and performances of different catalysts for photocatalytic selective oxidation of thioanisole.

Catalysts	Conditions	Light source	Time (h)	Conv.[a] (%)	Select.[a] (%)	Ref.
C, N-TNS (10 mg, 0.08 mmol TiO_2)	thioanisole (0.3 mmol), CH_3CN (5 mL), air, rt.	300 W Xe lamp (350 < λ < 780 nm)	6	100	95.0	This work
P25 (10 mg, 0.13 mmol)	thioanisole (0.3 mmol), CH_3CN (5 mL), air, rt.	300 W Xe lamp (350 < λ < 780 nm)	6	29.3	92.2	This work
h-LZU1 (10 mg)	thioanisole (0.3 mmol), CH_3CN (10 mL), air, 30 °C.	visible light source: 300 W Xe lamp (380 < λ < 780 nm)	22	100	92.6	7
TiO_2 (40 mg)	thioanisole (0.3 mmol), triethylamine (redox mediator, 0.03 mmol), CH_3OH (5 mL), O_2 (0.1 MPa), 25 °C.	300 W Xe lamp (λ > 400 nm)	10	84	92	8
Co-N-TiO_2 (40 mg)	thioanisole (0.3 mmol), triethylamine (redox mediator, 0.06 mmol), CH_3OH (5 mL), O_2, rt.	300 W Xe lamp (λ > 420 nm)	12	76.4	92.85	9
C_{60}/g-C_3N_4 (4 wt%, 30 mg)	thioanisole (0.2 mmol), CH_3OH (5 mL), O_2, 25 °C.	Xe lamp (1 W cm^{-2}, λ > 400 nm)	6	99.9	100	10
Ir-Zr MOF (4 mol %, based on Ir, 14.8 mg)	thioanisole (0.25 mmol), CH_3CN (4 mL), O_2, rt.	100 W blue LED	18	79[b]	-	11

[a] Conversion (Conv.) and selectivity (Select.) were determined by ^1H NMR.

[b] The yield of benzyl methyl sulfoxide.

Table S3. Effect of scavengers on thioanisole oxidation catalyzed by C, N-TNS.[a]

Entry	Scavengers	Quenching group	Conv. (%)[b]	Select. (%)[b]
1	beta-carotene	$^1O_2$	31.4	95.0
2	BQ	$O_2^{\bullet-}$	58.0	90.6

[a]Reaction conditions: 10 mg catalyst, 5 mL acetonitrile, 0.3 mmol thioanisole, 2 equivalent of scavenger, 6 h, 300 W Xe lamp ($350 < \lambda < 780$ nm). [b] Conv. and Select. were determined by ^{1}H NMR.

The conversion of thioanisole at 6 h drops from 100% to 31.4% in the presence of beta-carotene, which suggests that $^1O_2$ is present in the reaction system and serves as an ROS for the photocatalytic oxidation of thioanisole. With BQ as a scavenger to capture $O_2^{\bullet-}$, the conversion of thioanisole at 6 h decreases to 58.0%. The results indicate that $^1O_2$ and $O_2^{\bullet-}$ are the ROS for the photocatalytic oxidation of sulfides and the main ROS in the photocatalytic reactions is $^1O_2$.

References

1. G. P. Dai, S. Q. Liu, Y. Liang, H. J. Liu and Z. C. Zhong, *J. Mol. Catal. A: Chem.*, 2013, **368-369**, 38-42.
2. J. Yang, Y.-L. Jiang, L.-J. Li, E. Muhire and M.-Z. Gao, *Nanoscale*, 2016, **8**, 8170-8177.
3. X. N. Tan, J. L. Zhang, D. X. Tan, J. B. Shi, X. Y. Cheng, F. Y. Zhang, L. F. Liu, B. X. Zhang, Z. Z. Su and B .X. Han, *Nano Res.*, 2019, **12**, 1967-1972.
4. V. Etacheri, M. K. Seery, S. J. Hinder and S. C. Pillai, *Chem. Mater.*, 2010, **22**, 3843-3853.
5. A. V. Abega, H. M. Ngomo, I. Nongwe, H. E. Mukaya, P.-M. A. K. Sone and X. Y. Mbianda, *Synth. Met.*, 2019, **251**, 1-14.
6. A. M. Katzenmeyer, J. Canivet, G. Holland, D. Farrusseng and A. Centrone, *Angew. Chem., Int. Ed.*, 2014, **53**, 2852-2856.
7. L. F. Liu, B. X. Zhang, X. N. Tan, D. X. Tan, X. Y. Cheng, B. X. Han and J. L. Zhang, *Chem. Commun.*, 2020, **56**, 4567-4570.
8. X. J. Lang, W. Hao, W. R. Leow, S. Z. Li, J. C. Zhao and X .D. Chen, *Chem. Sci.*, 2015, **6**, 5000-5005.
9. M. M. Zou, L. Feng, T. Thomasc and M. H. Yang, *Catal. Sci. Technol.*, 2017, **7**, 4182-4192.
10. X. Chen, K. J. Deng, P. Zhou and Z. H. Zhang, *ChemSusChem*, 2018, **11**, 2444-2452.
11. L.-Q. Wei and B.-H. Ye, *ACS Appl. Mater. Interfaces*, 2019, **11**, 41448-41457.